processes

MDPI

Review

A Review of the Thermochemical Behaviour of Fluxes in Submerged Arc Welding: Modelling of Gas Phase Reactions

Theresa Coetsee * and Frederik De Bruin

Department of Materials Science and Metallurgical Engineering, University of Pretoria, Pretoria 0002, South Africa
* Correspondence: theresa.coetsee@up.ac.za

Abstract: This review is focused on the thermochemical behaviour of fluxes in submerged arc welding (SAW). The English-language literature from the 1970s onwards is reviewed. It was recognised early on that the thermochemical behaviour of fluxes sets the weld metal total ppm O and the element transfer extent from the molten flux (slag) to the weld pool. Despite the establishment of this link between the flux-induced oxygen potential and element transfer, it is also well accepted that the slag–metal equilibrium does not control SAW process metallurgy. Instead, the gas phase must be taken into account to better describe SAW process metallurgy equilibrium calculations. This is illustrated in the gas–slag–metal equilibrium simulation model developed by Coetsee. This model provides improved accuracy in predicting the weld metal total ppm O values as compared to the empirical trend of Tuliani et al. Recent works on the application of Al metal powder with alloying metal powders provide new insights into the likely gas phase reactions in the SAW process and the modification of the flux oxygen behaviour via Al additions. Aluminium may lower the partial oxygen pressure in the arc cavity, and aluminium also lowers the partial oxygen pressure at the weld pool–slag interface. The weld metal total ppm O is lowered with the addition of aluminium in SAW, but not to the same extent as would be expected from steelmaking ladle metallurgy de-oxidation practice when using Al as de-oxidiser. This difference indicates that slag–metal equilibrium is not maintained in the SAW process.

Keywords: modelling; flux; welding; SAW; gas; thermodynamics; oxygen; aluminium; basicity; slag; weld metal

Citation: Coetsee, T.; De Bruin, F. A Review of the Thermochemical Behaviour of Fluxes in Submerged Arc Welding: Modelling of Gas Phase Reactions. *Processes* **2023**, *11*, 658. https://doi.org/10.3390/pr11030658

Academic Editors: Chin-Hyung Lee and Sergio Bobbo

Received: 8 January 2023
Revised: 8 February 2023
Accepted: 20 February 2023
Published: 22 February 2023

1. Introduction

The research and development of submerged arc welding (SAW) has a long history in excess of 100 years [1]. SAW played a major role in World War II in the ship and tank building industries [1]. Many important research works were published in languages other than English since texts on SAW development can be traced to 1892 in Russia, and development continued in other non-English-speaking countries [1]. This review is focused on studies published in the open English literature from the 1970s and onwards.

The SAW process consists of complex interactions of physical, electrical, and chemical effects in the arc cavity [1,2]. The SAW process is started by striking the arc between the welding head and the base plate under the cover of a bed of raw unmelted granular flux. The arc cavity is formed by a layer of raw unmelted flux covering a layer of molten flux (slag), which in turn covers the arc to form the arc cavity. The arc cavity encapsulates the arc plasma, the weld wire tip, and the gasses emanating from the arc. Weld wire and flux are continuously fed through the welding head arrangement as it moves along the weld. As the weld wire is melted, the molten weld wire metal droplets are transferred from the weld wire into the weld pool. The welding machine input selections of current, weld wire diameter, voltage, travel speed, current polarity, and electrode (weld wire) extension are very important in setting the weld energy input, and these parameters also influence

element transfer in the SAW process [1,3,4]. However, the flux chemistry has an outsized effect on the SAW process metallurgy [1,3,4]. The welding flux performs several intricate process functions. For example, it forms a slag layer around the arc plasma to shield the arc from atmospheric oxygen and nitrogen, it limits weld metal hydrogen absorption from moisture, it limits arc energy losses from the arc to the environment by forming an opaque low-conductivity slag boundary around the arc cavity, and it transfers alloying elements to the weld metal [3,4].

Fluxes may be classified according to preparation methods, such as agglomerated, fused, or mechanically mixed fluxes [4]; according to the element transfer behaviour from the flux to the weld metal as neutral flux, active flux, or alloy flux [4]; or in terms of chemical formulation categories, for example, fluoride basic flux, aluminate basic flux, etc. [5]. Despite the different flux classification options, the one major consideration in SAW is the weld metal total oxygen content resulting from the use of a particular flux formulation. The weld metal total oxygen content must be controlled within limits to ensure acceptable materials properties of the weld, as applied in a specific materials application. For example, high impact toughness is maintained in carbon steel weld metal if the total oxygen content is within the band of 200 ppm to 500 ppm O, with both too low or too high total ppm O content resulting in poor weld metal impact toughness [6]. In addition, some oxygen is required in the weld pool to form particular oxide inclusions (e.g., TiO_2), which form preferred nucleation sites for acicular ferrite (AF). AF is the preferred microstructure to improve the carbon steel weld metal materials properties of impact toughness and tensile strength [7,8]. In 1969, Tuliani et al. [9] published the widely used empirically determined relationship trend line of the flux composition basicity index, the BI, as expressed in Equation (1), vs. the weld metal total ppm O. Based on this trend line, at flux BI values in excess of 1.5, the weld metal total ppm O is constant at 250 ppm O [9]. High flux basicity typically implies a relatively higher proportion of CaF_2 in the flux. The weld metal hydrogen content is also minimised at high flux basicities due to the higher CaF_2 addition in the flux [9,10].

$$\mathrm{BI} = \frac{\%CaF_2 + \%CaO + \%MgO + \%BaO + \%SrO + \%Na_2O + \%K_2O + \%Li_2O + 0.5(\%MnO + \%FeO)}{\%SiO_2 + 0.5(\%Al_2O_3 + \%TiO_2 + \%ZrO_2)} \quad (1)$$

The two main alloying elements in carbon steel SAW are manganese and silicon. Because these elements are lost from the weld pool during the welding process, the flux typically contains MnO and SiO_2 to limit Mn and Si loss to the slag, and Si and Mn are added from the weld wire to the weld pool [3,4]. Element micro-alloying of the weld pool from the flux can also be performed in ppm quantities. One example is the addition of Ti to the weld pool from the flux in ppm quantities to react with the oxygen in the weld pool to form TiO_2, which induces an acicular ferrite structure in the weld metal [3,4,7,8]. Therefore, the flux chemistry is formulated to achieve targeted element transfer levels from the slag to the weld metal, as illustrated in several studies [11–13].

Besides the design of a flux formulation for specific element transfer to the weld pool, control of the weld metal total oxygen content, and limiting hydrogen pick-up into the weld metal, the flux is also formulated to achieve certain physico-chemical properties in the slag. For example, the slag viscosity and surface tension are influenced by CaF_2, as the F^- serves as a network modifier anion [14]. Fluoride minerals, typically CaF_2, are added to the flux to ensure that the flux melts at approximately 50 °C lower than the weld metal [15]. This allows the flux to solidify after the weld pool (molten steel) has solidified, so that the maximum possible period of time is allowed for chemical reactions between the flux and the weld pool. An increased reaction time between the weld pool and the slag is very important to allow the removal of oxide inclusions from the weld pool. This reaction time extension is required because the inclusions must first float out of the weld pool to the slag–weld pool interface, where the inclusions are subsequently absorbed into the slag to ensure cleaner weld metal containing less oxide inclusions [16]. The maximum weld pool temperature has been reported to be 2000 °C [10,17,18]. As discussed extensively in the literature, flux is formulated to form a “short” or “long” slag, depending on the

welding application [19,20]. Most fused fluxes form "short" slags since their compositions are selected close to the multi-component system's eutectic composition [20]. The result is that the difference between the slag liquidus temperature and the slag solidus temperature is small, and the slag transitions over a small temperature interval from a fluid state to a viscous state [19–21]. Most agglomerated fluxes form "long" slags with the opposite melt characteristics compared to a "short" slag [14]. The addition of CaF_2 to the oxides in the flux results in a drastic lowering of the oxide only slag's liquidus and solidus temperatures [14,20,22]. Recent studies from different research groups are available on SAW flux development, linking the physico-chemical properties of the molten flux (slag) to flux input compositions via regression studies and fundamental slag structure studies, for example [23,24]. For wider overview type publications on the historically accepted SAW metallurgy, its thermodynamics interpretation, and the chemical and physical behaviours of fluxes, the reader is referred to well-referenced texts in [25,26].

Although the physico-chemical properties of the slag formed from the flux are important in flux design, the first concern in flux design is the weld metal total ppm O. The flux oxygen behaviour sets both the weld metal total ppm O and the element transfer extent between the molten flux (slag) and the weld pool. The following section explores the link between flux formulation and weld metal total ppm O.

2. The Importance of Oxygen in SAW

The de-oxidation of liquid steel in ladle metallurgy is often equated to SAW process metallurgy to explain the transfer of elements between the molten flux (slag) and the molten steel weld pool [10,11,16,27]. The justification for this approach is well discussed by Chai and Eagar [10]. The authors also explain that it is well accepted that thermodynamic equilibrium is not attained between the slag and metal in flux-shielded welding. However, the slag–metal equilibrium calculations for an effective chemical reaction temperature of 2000 °C correlate with measured post-weld slag and metal chemistries for the major carbon steel alloying elements in SAW, namely Si and Mn [10].

The link between element transfer to the weld pool and the weld pool molten steel oxygen content is made in terms of steelmaking reactions. For example, the element transfer of Mn between the slag and the weld pool is often written, as in Reaction (2), for the reaction of Mn dissolved in steel reacting with oxygen dissolved in steel to form liquid MnO in the slag [10]. The slag–metal reaction equilibrium, as represented in Equation (3), can then be shifted by changing the activity of MnO in the slag. However, the starting value of the dissolved oxygen in the weld pool is unknown, and therefore this approach has no predictive capability. Therefore, based on the BI of the planned flux formulation, the value of the final weld metal total ppm O from the Tuliani et al. [9] trend line is used as the input for the weld pool dissolved oxygen in Equation (3). Then, in combination with the known value of the MnO activity in the starting slag from the flux formulation, the predicted equilibrium value of %Mn in the weld pool at 2000 °C is calculated from Equation (3). Based on the flux chemistry, the activity of MnO may be changed to at least steer Reaction (2) to the left to increase the Mn transfer from the slag to the weld pool.

$$\underline{Mn} + \underline{O} \leftrightarrow MnO(l) \quad (2)$$

$$K = \frac{a_{MnO}}{a_{Mn}a_O} \quad (3)$$

a_{MnO} = activity of MnO in slag

a_O and a_{Mn} = Henrian activity of O and Mn in steel.

In a series of papers by Mitra and Eagar, an extensive model was developed [17,18,28] based on the neutral point concept, which is the flux composition at which no element transfer occurs between the slag and the weld pool for a particular alloying element [10]. The neutral point, expressed in the model as the mass% of an alloying element in the weld metal for the neutral point slag composition, is then shifted in the model with the inclusion of kinetic factors, weld bead geometry parameters, and the changed flux chemistry oxide

activity [17,18,28]. The limitation in all these calculations is that the starting point is still the empirical relationship of the flux BI vs. the final weld metal total ppm O from Tuliani et al. [9]. This correlates with the recommendation from the PhD thesis of Mitra that future work should target model development to predict the weld metal total ppm O [29]. In addition to the above model development efforts, many studies were reported in which the process metallurgy of the SAW process was clarified, as discussed below.

The initial level of total ppm O entering the weld pool via molten weld wire droplets was measured to be 2000–3000 ppm O [30,31]. It has been shown experimentally that the dissociation of oxides in the molten flux (slag) at the high temperatures prevailing in the arc cavity is the only source of this 2000–3000 ppm O [32]. Therefore, this initial large quantity of oxygen added to the weld pool must be decreased to acceptable levels of 200 ppm O to 500 ppm O before the weld pool is solidified. This target total ppm O level in weld metal is much higher than the equilibrium ppm O measured as dissolved oxygen in carbon steel de-oxidation experiments, for example, 10 ppm O at 0.1% Al at 1600 °C [33]. Therefore, as confirmed in prior studies, the slag–metal equilibrium does not control the process metallurgy in SAW. Therefore, the mechanism of oxygen control in the weld pool is clearly dependant on reactions other than only the ladle metallurgy based reactions.

Since the SAW process takes place at high temperatures, especially in the arc cavity at 2000 °C–2500 °C, it would be reasonable to expect that the arc plasma stability order of oxides in the flux also follows the oxide thermodynamic stability order [10,17,18]. However, welding experiments were used to show the unique arc plasma stability order for the oxides that are typically used in SAW flux formulations. These experiments consisted of welding tests conducted under argon gas by using different oxide–CaF_2 flux mixtures and then measuring the weld metal total ppm O [32]. A higher weld metal total ppm O confirmed that the particular metal oxide in the oxide-CaF_2 flux is less stable in the arc because the oxide dissociated in the arc plasma to release oxygen. The oxide arc plasma stability order from the most stable oxide to the least stable oxide is: CaO, K_2O, Na_2O, TiO_2, Al_2O_3, MgO, SiO_2, and MnO [32]. Consequently, the weld metal total ppm O can be lowered by adding more CaF_2 into the flux mixture to dilute the quantity of low-stability oxides in the molten flux (slag).

The effect of fluorides in the flux is to lower the P_{O2} in the arc cavity by forming fluorine-based compounds via reactions similar to Reaction (4) between SiO_2 and CaF_2 [32,34]. Similarly, the P_{H2} is lowered to limit hydrogen pick-up into the weld metal [35,36]. Hydrogen pick-up into the weld pool is also limited by reactions of water vapour and CaF_2, according to Reaction (5), and by formulating the flux chemistry for an increased hydrogen dissolution capacity [34–36].

$$SiO_2(l) + 2CaF_2(g) \leftrightarrow 2CaO(s) + SiF_4(g) \quad (4)$$

$$H_2O(g) + CaF_2(g) \leftrightarrow CaO(s) + 2HF(g) \quad (5)$$

From the above discussion of studies reported in the literature, it is clear that the gas phase in the arc cavity plays an important role in the process metallurgy of SAW and that the gas–slag–metal equilibrium should be used instead of the slag–metal equilibrium to model the SAW process adequately. An indication of a reaction between the arc cavity gas phase and the weld pool is given in previous studies which show that the excessive quantity of oxygen transferred via gas phase reactions in the arc cavity (2000–3000 ppm) reacts with the molten steel at the arc plasma–weld pool interface to form FeO [18,25,37,38]. This FeO is incorporated into the slag, as shown in the FeO content analysed in the post-weld slags [27,37,38]. The correlation of increased FeO in the molten flux with increased weld metal total ppm O is well established, and the slag FeO content serves as an indicator of the oxygen potential prevailing at the molten flux–weld pool interface [27,37,38]. Because most fluxes contain less than 2 mass% iron oxides, and the slag FeO is formed during welding, and the FeO content in the slag is not at the slag–metal equilibrium, these factors mean that the slag FeO content has no predictive capability in linking flux chemistry to the weld metal total ppm O [10,27,38].

3. Thermochemical Modelling

Given the lack of gas phase incorporation in previous models and the clear importance of the gas phase in SAW process metallurgy, the gas–slag–metal equilibrium simulation model of the SAW process was developed by Coetsee, with the model details described in Coetsee et al. [38]. The availability of thermochemical software platforms makes this type of multi-phase thermodynamic calculation accessible to more researchers. In this case, FactSage 7.3 thermochemical software was used to simulate the SAW process [39]. This model calculates the weld metal composition via the gas–slag–metal equilibrium for different input flux chemistries [38]. The required inputs are the chemical compositions of the flux, wire, and base plate and the proportions of these input materials. The model outputs consist of the gas phase, weld metal, and slag phases in terms of composition, masses, and thus also fugacities. The welding parameters of voltage, current, and welding speed set the energy input level in the arc cavity and weld pool and may be represented in the model by the effective chemical reaction equilibrium temperature of 2000 °C, as specified in previous studies [10,17,18,34]. However, the best calculation results are obtained when utilising 2100 °C as the effective equilibrium temperature [38].

The model performance was verified against a set of bead-on-plate welding tests performed with different commercial agglomerated fluxes of wide-ranging BI values of 0.5 to 3.0 [38]. The measured weld metal total ppm O values ranged widely from 296 ppm O to 678 ppm O [38]. The importance of an accurate description of the agglomerated flux mineral chemistry with respect to the presence of $CaCO_3$ was illustrated as well [40]. This model provides improved accuracy in predicted weld metal total ppm O values compared to the empirical trend of Tuliani et al. [9], as shown in Figure 1 and Table 1. The error bars in Figure 1 for the analysed weld metal total ppm O values are for reference only, set at ±50 ppm O, even though the analysis uncertainty is ±10 ppm O. The model accuracy was also verified in comparison studies of the weld metal total ppm O to the model-calculated weld metal total ppm O from carbon steel weld metal studies in high heat input welding [41–43].

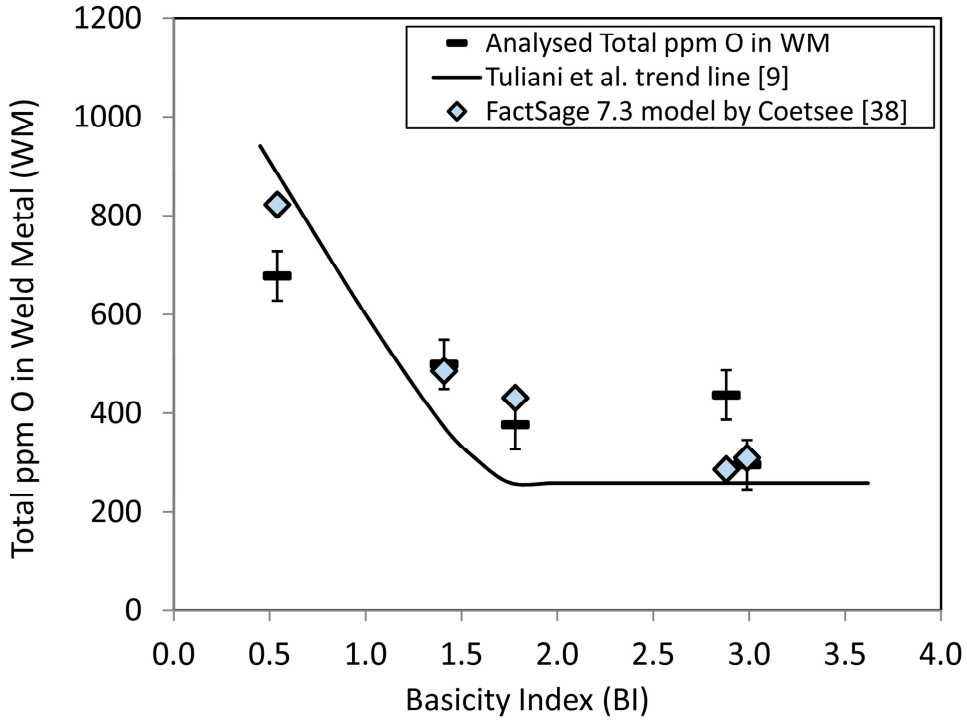

Figure 1. Total ppm O in weld metal vs. flux basicity index (BI): comparison of measured values vs. Tuliani et al. trend line vs. Coetsee FactSage 7.3 gas–slag–metal equilibrium simulation model [38].

Table 1. Total ppm O values in weld metal, as displayed in Figure 1.

BI	Measured Values [38]	Coetsee FactSage 7.3 Gas–Slag–Metal Equilibrium Simulation Model [38]	Tuliani et al. Trend Line [9]
3.0	296	310	259
2.9	437	287	259
1.8	377	431	259
1.4	499	486	377
0.5	678	822	941

4. New Insights into SAW Process Metallurgy from De-Oxidation with Al

The gas–slag–metal equilibrium model described in Section 3 was more recently applied to elucidate the role of aluminium de-oxidiser in the SAW process in terms of controlling the partial oxygen pressure at the weld pool–slag interface, as well as in the arc cavity via gas phase reactions [44–46]. This work spanned a series of papers on the application of Al powder with various combinations of alloying metal powders in SAW by using the same flux and input weld parameters [44–52]. The metal powders were applied in unconstrained format, meaning that the non-alloyed metal powders were not constrained in tubular wires, such as flux-cored and metal-cored wire. This work showed that the role of Al in the gas phase is to lower the partial oxygen pressure in the gas phase contained in the arc cavity by preferentially forming Al-fluorides. The elements with high oxygen affinity, such as Cr and Ti, are not easily transferred across the arc [4]. This work showed that the addition of Al as a de-oxidiser ensured that the metal powders of these elements (Cr and Ti) were not oxidised and lost to the slag [44–54].

Furthermore, because of the higher thermodynamic stability of Al-fluorides relative to the fluorides of the main elements contained in the welding fluxes, the less stable metal fluorides are easily transformed to metallic elements in the gas phase, similar to Reaction (6) for CrF_3(g) reacting with Al(g) [45,46]:

$$Al(g) + CrF_3(g) \leftrightarrow AlF_3(g) + Cr(g) \quad (6)$$

Therefore, the application of Al to lower the partial oxygen pressure in the arc cavity and at the slag–weld pool interface prevents the significant oxidation of high-oxygen-affinity elements such as Cr to prevent Cr oxidation and its loss to the slag in the form of oxides. In the arc cavity, the speciation of Cr is shifted to Cr(g) instead of CrF_3(g), as shown in Reaction (6), with some Cr element loss to the gas phase and slag. However, with Al addition the Cr yield to the weld pool is enhanced compared to Cr transfer from pre-alloyed powders and from Cr-containing flux [24,55,56].

The following discussion of our SAW process flow diagram in Figure 2 incorporates the findings and insights from the thermodynamic analyses of gas-based reactions for the application of Ni, Cr, and Al powders in unconstrained format [45,46]. Reaction steps A to E represent oxygen transfer steps from the slag to the weld pool due to the decomposition of oxides in the arc cavity, as determined in various well-accepted studies [24,27,30,31,34,38]. Reaction A, namely the reaction of Al_2O_3 with CaF_2(g) to form AlF_3(g) and CaO, is an example of the type of reaction typically written in texts on fluoride-based welding fluxes, similar to Reaction (4) above [32,34,57]. In our previous thermodynamic analyses of possible gas phase reactions, it was shown that reactions similar to reaction A in Figure 2 are thermodynamically less probable since the reaction of metal vapour with F_2 gas has much lower Gibbs free energy values for all the oxides typically encountered in SAW fluxes [44–46,52]. As already mentioned, an excessive initial quantity of oxygen of 2000–3000 ppm O is added to the weld pool via the molten weld wire droplets in the arc cavity gas phase [30,31]. The word "excessive" means that the ppm O in the weld pool exceeds the solubility limit of oxygen in liquid steel at the particular weld pool temperature. The arc only momentarily adds arc energy into the weld pool because the welding head moves forward along the

weld run. Therefore, the weld pool cools down quickly, with the result being that the weld pool temperatures decrease from the high arc plasma temperatures of 2000–2500 °C, causing a decrease in the weld pool oxygen solubility [10,17].

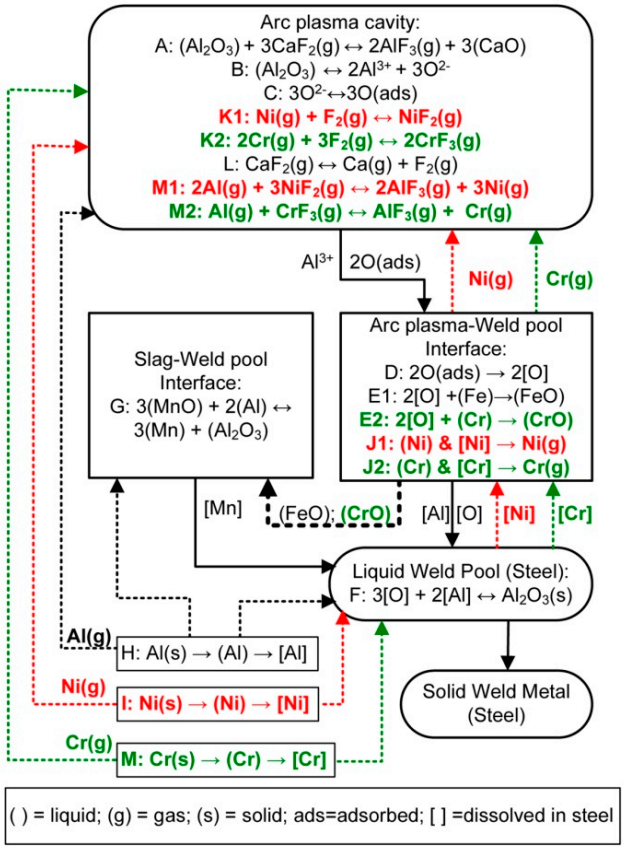

Figure 2. SAW reaction flow diagram with Al, Ni, and Cr powder additions [45].

This excessive quantity of oxygen transferred from the arc cavity to the weld pool reacts with the molten steel at the arc plasma–weld pool interface to form FeO (see reaction E in Figure 2). The FeO is then assimilated into the slag. The correlation of increased FeO in the post-weld slag with the increased weld metal total ppm O confirmed this oxygen transfer mechanism [27,37,38]. The oxygen potential that prevails at the molten flux–weld pool interface is represented by the quantity of FeO in the slag. In our work, we added Al as a de-oxidiser element to reduce the oxygen potential, which in turn resulted in a decreased FeO content in the slag [53,54]. Therefore, similar to reaction G for the aluminothermic reduction of MnO from the molten flux, FeO may also be reduced by aluminium. These aluminothermic reduction reactions reduce MnO, SiO_2, and FeO from the slag and release chemical energy in the form of heat into the weld pool because these are exothermic reactions [44–52]. This extra added heat can be used to melt and dissolve metal powder into the weld pool.

The reduced oxygen potential at the molten flux–weld pool interface prevents the oxidation of metallic Cr powder to the Cr-oxides, CrO and Cr_2O_3, and thereby prevents Cr loss to the slag. In the same way, the oxidation of Ni to NiO is prevented, even though Ni has a much lower affinity for oxygen than Cr. Since Cr has a high affinity for oxygen, the formation of CrO may occur at the arc plasma–weld pool interface (reaction E2). However, it is expected that this CrO would be reduced by aluminium according to a reaction similar to reaction G in Figure 2 [45,46,48,49,51]. In the same way, any loss of Ni as NiO into the slag can be prevented by the addition of Al to the weld pool. As displayed by reactions I and M, most of the added Ni and Cr metal powders are melted and dissolved into the

weld pool. Since there is an excess of Al added, some of the Al also directly dissolves into the weld pool (see reaction H).

The Gibbs free energy values of the individual reactions show that some Cr and Ni loss is possible due to Cr and Ni vaporisation and/or the subsequent reaction of chromium and nickel vapour with F_2 gas to form CrF_2(g), CrF_3(g), and NiF_2(g) [45,52]. This reaction sequence is marked in Figure 2 in red text as reactions J1 and K1 for nickel reactions and in green text as reactions J2 and K2 for chromium reactions. The source of F_2 gas is the dissociation of CaF_2(g) in the arc cavity via reaction L. The formation of F_2 gas in the arc cavity from the dissociation of CaF_2(g) in the arc plasma appears to be possible since Ca and F were analysed in the arc cavity gas phase when a CaF_2-based flux was used in SAW test runs [1,2].

As explained above for Reaction (6), Al vapour may react with the chromium and nickel fluorides CrF_2(g), CrF_3(g), and NiF_2(g) to transform these fluorides into Ni and Cr, as shown by reactions M1 and M2 in Figure 2. Cr and Ni can also be vaporised from the weld pool, at the arc plasma–weld pool interface, and from the unconstrained metal powders before the dissolution of the metal powders into the weld pool. The presence of Cr and Ni vapour in the gas–slag–metal powder equilibrium calculations confirms that Cr and Ni metal vapours may remain unreacted in the gas phase [45,52].

From the above discussion, it can be concluded that added Al powder plays a role in gas phase reactions by shifting chromium and nickel powders to the vapour phase instead of the oxidation of chromium and nickel powders to CrO, Cr_2O_3, and NiO by lowering the gas phase P_{O2} in the arc cavity [45,52]. This agrees with previous studies that showed lowered partial oxygen pressures from Al metal powder added to the flux [58]. Even in the absence of Al additions, it was shown that Al transferred to the weld pool from Al_2O_3-containing flux via the gas phase in the arc cavity [57].

It is clear that the added Al de-oxidiser plays an important role in the gas phase reactions, especially in lowering the partial oxygen pressure in the arc cavity. However, the final deciding factor for the oxidation state of Cr and Ni is the partial oxygen pressure at the molten flux–weld pool interface because this reaction interface remains active until the weld pool solidifies. The importance of this action of Al at the molten flux–weld pool interface is that the transfer of Cr and Ni into the weld pool is enhanced without interfering with oxygen transfer from the arc plasma to the weld pool. As mentioned before, if the Al de-oxidiser equilibrium prevailed via the Al/Al_2O_3 slag–metal equilibrium reaction as observed in ladle metallurgy, then the weld metal total ppm O should be very low at 10 ppm O at 0.1% Al at 1600 °C [33]. Much higher weld metal total ppm O values of 180 ppm O to 509 ppm O were measured in our work with Al de-oxidiser in SAW, even at the high %Al in the weld metal at 1.0% Al to 6.8% Al, confirming that oxygen transfer from the arc cavity via the arc plasma–weld pool interface was maintained.

5. Conclusions

1. Although it is well accepted that the slag–metal equilibrium does not hold for the SAW process, element transfer in SAW is still described in terms of this approach.
2. The main reason for this deficiency is the absence of a gas-phase-based model to predict the weld metal total ppm O as a function of flux composition. The only correlation between the weld metal total ppm O and flux chemistry used in industry is the empirical correlation of Tuliani et al. as published in 1969.
3. The importance of gas phase reactions in the SAW process is illustrated in the gas–slag–metal equilibrium simulation model developed by Coetsee. This model provides improved accuracy in predicted weld metal total ppm O values compared to the empirical trend of Tuliani et al.
4. Recent works on the application of Al metal powder with alloying metal powders provide new insights into the likely gas phase reactions in the SAW process, and the modification of the flux oxygen behaviour via Al additions. Al in the arc cavity may

lower the partial oxygen pressure in the arc cavity, and Al also lowers the partial oxygen pressure at the weld pool–slag interface.
5. The weld metal total ppm O is lowered with the addition of Al in SAW, but not to the same extent as would be expected from steelmaking ladle metallurgy Al de-oxidation practice, indicating that slag–metal equilibrium is not maintained in the SAW process.
6. Aluminium in the arc cavity may lower the partial oxygen pressure in the arc cavity, and aluminium also lowers the partial oxygen pressure at the weld pool–slag interface without interfering with oxygen transfer from the arc plasma to the weld pool.

Author Contributions: F.D.B. and T.C. interpreted the data together and prepared the manuscript together. All authors have read and agreed to the published version of the manuscript.

Funding: This research was funded in part by the University of Pretoria.

Data Availability Statement: The data sets presented in this study are available upon reasonable request from the corresponding author indicated on the first page.

Conflicts of Interest: The authors declare no conflict of interest. The funders had no role in the design of the study; in the collection, analyses, or interpretation of data; in the writing of the manuscript; or in the decision to publish the results.

References

1. Sengupta, V.; Havrylov, D.; Mendez, P.F. Physical phenomena in the weld zone of submerged arc welding—A Review. *Weld. J.* **2019**, *98*, 283–313.
2. Gött, G.; Gericke, A.; Henkel, K.-M.; Uhrlandt, D. Optical and spectroscopic study of a submerged arc welding cavern. *Weld. J.* **2016**, *95*, 491–499.
3. Linnert, G.E. *Welding Metallurgy-Carbon and Alloy Steels, Volume I-Fundamentals*, 4th ed.; American Welding Society (AWS): Miami, FL, USA, 1994; pp. 706–758.
4. O'Brien, A. *Welding Handbook—Welding Processes, Part 1*, 9th ed.; American Welding Society (AWS): Miami, FL, USA, 2004; Volume 2.
5. Kumar, A.; Singh, H.; Maheshwari, S. A review study of Submerged Arc Welding fluxes. *I-Manag. J. Mech. Eng.* **2013**, *3*, 44–52. [CrossRef]
6. Dallam, C.B.; Liu, S.; Olson, D.L. Flux composition dependence of microstructure and toughness of submerged arc HSLA weldments. *Weld. J.* **1985**, *64*, 140–152.
7. Koseki, T.; Thewlis, G. Overview Inclusion assisted microstructure control in C–Mn and low alloy steel welds. *Mat. Sci. Technol.* **2005**, *21*, 867–879. [CrossRef]
8. Sarma, D.S.; Karasev, A.V.; Jönsson, P.G. On the Role of Non-metallic Inclusions in the Nucleation of Acicular Ferrite in Steels. *ISIJ Int.* **2009**, *49*, 1063–1074. [CrossRef]
9. Tuliani, S.S.; Boniszewski, T.; Eaton, N.F. Notch toughness of commercial submerged arc weld metal. *Weld. Met. Fabr.* **1969**, *37*, 327–339.
10. Chai, C.S.; Eagar, T.W. Slag-metal equilibrium during submerged arc welding. *Metall. Trans. B* **1981**, *12*, 539–547. [CrossRef]
11. Palm, J.H. How fluxes determine the metallurgical properties of Submerged Arc Welds. *Weld. J.* **1972**, *51*, 358–360.
12. Paniagua-Mercado, A.M.; López-Hirata, V.M.; Muñoz, M.L.S. Influence of the chemical composition of flux on the microstructure and tensile properties of submerged-arc welds. *J. Mater. Process. Technol.* **2005**, *169*, 346–351. [CrossRef]
13. Bang, K.-S.; Park, C.; Jung, H.-C.; Lee, J.-B. Effects of flux composition on the element transfer and mechanical properties of weld metal in submerged arc welding. *Met. Mater. Int.* **2009**, *15*, 471–477. [CrossRef]
14. Mills, K.C. Structure and Properties of Slags Used in the Continuous Casting of Steel: Part 1 Conventional Mould Powders. *ISIJ Int.* **2016**, *56*, 1–13. [CrossRef]
15. Singh, B.; Khan, Z.A.; Siddiquee, A.N. Effect of flux composition on element transfer during Submerged Arc Welding (SAW): A literature review. *Int. J. Curr. Res.* **2013**, *5*, 4181–4186.
16. Kluken, A.O.; Grong, Ø. Mechanisms of inclusion formation in Al−Ti−Si−Mn deoxidized steel weld metals. *Metall. Trans. A* **1989**, *20*, 1335–1349. [CrossRef]
17. Mitra, U.; Eagar, T.W. Slag-metal reactions during welding: Part I. Evaluation and reassessment of existing theories. *Metall. Trans. B* **1991**, *22*, 65–71. [CrossRef]
18. Mitra, U.; Eagar, T.W. Slag-metal reactions during welding: Part II. Theory. *Metall. Trans. B* **1991**, *22*, 73–81. [CrossRef]
19. Sokolsky, V.E.; Roik, O.S.; Davidenko, A.O.; Kazimirov, V.P.; Lisnyak, V.V.; Galinich, V.I.; Goncharov, I.A. The phase evolution at high-temperature treatment of the oxide-fluoride ceramic flux. *Res. J. Chem. Sci.* **2014**, *4*, 71–77.
20. Davidenko, A.O.; Sokolsky, V.E.; Lisnyak, V.V.; Roik, O.S.; Goncharov, I.A.; Galinich, V.I. The effect of spinel formation in the ceramic welding fluxes on the properties of molten slag. *Res. J. Chem. Sci.* **2015**, *5*, 23–31.

21. Golovko, V.V.; Potapov, N.N. Special features of agglomerated (ceramic) fluxes in welding. *Weld. Int.* **2011**, *25*, 889–893. [CrossRef]
22. Coetsee, T. Phase chemistry of Submerged Arc Welding (SAW) fluoride based slags. *J. Mater. Res. Technol.* **2020**, *9*, 9766–9776. [CrossRef]
23. Sharma, L.; Kumar, J.; Chhibber, R. Experimental investigation on high temperature wettability and structural bahaviour of SAW fluxes using MgO–TiO_2–SiO_2 and Al_2O_3–MgO–SiO_2 flux system. *Ceram. Int.* **2020**, *46*, 5649–5657. [CrossRef]
24. Zhang, Y.; Coetsee, T.; Yang, H.; Zhao, T.; Wang, C. Structural roles of TiO_2 in CaF_2-SiO_2-CaO-TiO_2 submerged arc welding fluxes. *Metall. Trans. B* **2020**, *51*, 1947–1952. [CrossRef]
25. Olson, D.; Liu, S.; Frost, R.; Edwards, G.; Fleming, D. Nature and Behavior of Fluxes Used for Welding. In *ASM Handbook*; ASM International: Almere, The Netherlands, 1993; Volume 6, pp. 55–63.
26. Natalie, C.A.; Olson, D.L.; Blander, M. Physical and Chemical Behavior of Welding Fluxes. *Annu. Rev. Mater. Sci.* **1986**, *16*, 389–413. [CrossRef]
27. Mitra, U.; Eagar, T.W. Slag Metal Reactions during Submerged Arc Welding of Alloy Steels. *Metall. Trans. A* **1984**, *15*, 217–227. [CrossRef]
28. Mitra, U.; Eagar, T.W. Slag-metal reactions during welding: Part III. Verification of the Theory. *Metall. Trans. B* **1991**, *22*, 83–100. [CrossRef]
29. Mitra, U. Kinetics of Slag Metal Reactions during Submerged Arc Welding of Steel. Ph.D. Thesis, Massachusetts Institute of Technology, Cambridge, MA, USA, 1984; p. 205.
30. Polar, A.; Indacochea, J.E.; Blander, M. Electrochemically generated oxygen contamination in submerged arc welding. *Weld. J.* **1990**, *69*, 68–74.
31. Lau, T.; Weatherly, G.C.; McLean, A. The sources of oxygen and nitrogen contamination in submerged arc welding using CaO-Al_2O_3 based fluxes. *Weld. J.* **1985**, *64*, 343–347.
32. Chai, C.S.; Eagar, T.W. Slag metal reactions in binary CaF_2-metal oxide welding fluxes. *Weld. J.* **1982**, *61*, 229–232.
33. Jung, I.-H.; Decterov, S.A.; Pelton, A.D. Computer Applications of Thermodynamic Databases to Inclusion Engineering. *ISIJ Int.* **2004**, *44*, 527–536. [CrossRef]
34. Eagar, T.W. Sources of weld metal oxygen contamination during submerged arc welding. *Weld. J.* **1978**, *57*, 76–80.
35. Du Plessis, J.; Du Toit, M.; Pistorius, P.C. Control of diffusible weld metal hydrogen through flux chemistry modification. *Weld. J.* **2007**, *86*, 273–280.
36. Park, J.-Y.; Chang, W.-S.; Sohn, I. Effect of MnO to hydrogen dissolution in CaF_2–CaO–SiO_2 based welding type fluxes. *Sci. Techol. Weld. Join.* **2012**, *17*, 134–140. [CrossRef]
37. Indacochea, J.E.; Blander, M.; Christensen, N.; Olson, D.L. Chemical reactions during submerged arc welding with FeO-MnO-SiO_2 fluxes. *Metall. Trans. B* **1985**, *16*, 237–245. [CrossRef]
38. Coetsee, T.; Mostert, R.J.; Pistorius, P.G.H.; Pistorius, P.C. The effect of flux chemistry on element transfer in Submerged Arc Welding: Application of thermochemical modelling. *J. Mater. Res. Technol.* **2021**, *11*, 2021–2036. [CrossRef]
39. Bale, C.W.; Bélisle, E.; Chartrand, P.; Decterov, S.A.; Eriksson, G.; Gheribi, A.E.; Hack, K.; Jung, I.-H.; Kang, Y.-B.; Melançon, J.; et al. Reprint of: FactSage thermochemical software and databases, 2010–2016. *Calphad* **2016**, *55*, 1–19. [CrossRef]
40. Coetsee, T. Gas-slag-metal equilibrium simulation model of the Submerged Arc Welding process-the effect of flux chemistry on carbon steel weld metal oxygen content. In Proceedings of the THANOS International Conference 2022, Randburg, South Africa, 28–29 September 2022; pp. 23–33.
41. Zhang, J.; Coetsee, T.; Basu, S.; Wang, C. Impact of gas formation on the transfer of Ti and O from TiO_2-bearing basic-fluoride fluxes to submerged arc welded metals: A thermodynamic approach. *Calphad* **2020**, *71*, 102195. [CrossRef]
42. Zhang, J.; Wang, C.; Coetsee, T. Assessment of Weld Metal Compositional Prediction Models Geared Towards Submerged Arc Welding: Case Studies Involving CaF_2-SiO_2-MnO and CaO-SiO_2-MnO Fluxes. *Metall. Mater. Trans. B* **2021**, *52*, 2404–2415. [CrossRef]
43. Zhang, J.; Wang, C.; Coetsee, T. Thermodynamic Evaluation of Element Transfer Behaviors for Fused CaO-SiO_2-MnO Fluxes Subjected to High Heat Input Submerged Arc Welding. *Metall. Mater. Trans. B* **2021**, *52*, 1937–1944. [CrossRef]
44. Coetsee, T.; De Bruin, F. Application of Unconstrained Cobalt and Aluminium Metal Powders in the Alloying of Carbon Steel in Submerged Arc Welding: Thermodynamic Analysis of Gas Reactions. *Appl. Sci.* **2022**, *12*, 8472. [CrossRef]
45. Coetsee, T.; De Bruin, F. Aluminium-Assisted Alloying of Carbon Steel in Submerged Arc Welding with Al-Cr-Ni Unconstrained Metal Powders: Thermodynamic Interpretation of Gas Reactions. *Processes* **2022**, *10*, 2265. [CrossRef]
46. Coetsee, T.; De Bruin, F. Modification of Flux Oxygen Behaviour via Co-Cr-Al Unconstrained Metal Powder Additions in Submerged Arc Welding: Gas Phase Thermodynamics and 3D Slag SEM Evidence. *Processes* **2022**, *10*, 2452. [CrossRef]
47. Coetsee, T.; De Bruin, F.J. Improved titanium transfer in Submerged Arc Welding of carbon steel through aluminium addition. *Miner. Process. Extr. Metall. Rev.* **2021**, *43*, 771–774. [CrossRef]
48. Coetsee, T.; De Bruin, F. Reactions at the molten flux-weld pool interface in submerged arc welding. *High Temp. Mater. Process.* **2021**, *40*, 421–427. [CrossRef]
49. Coetsee, T.; De Bruin, F. Application of Copper as Stabiliser in Aluminium Assisted Transfer of Titanium in Submerged Arc Welding of Carbon Steel. *Processes* **2021**, *9*, 1763. [CrossRef]
50. Coetsee, T.; De Bruin, F. Chemical Interaction of Cr-Al-Cu Metal Powders in Aluminum-Assisted Transfer of Chromium in Submerged Arc Welding of Carbon Steel. *Processes* **2022**, *10*, 296. [CrossRef]

51. Coetsee, T.; De Bruin, F. Aluminium-Assisted Alloying of Carbon Steel in Submerged Arc Welding: Application of Al-Cr-Ti-Cu Unconstrained Metal Powders. *Processes* **2022**, *10*, 452. [CrossRef]
52. Coetsee, T.; De Bruin, F. Aluminium Assisted Nickel Alloying in Submerged Arc Welding of Carbon Steel: Application of Unconstrained Metal Powders. *Appl. Sci.* **2022**, *12*, 5392. [CrossRef]
53. Coetsee, T.; De Bruin, F. Insight into the Chemical Behaviour of Chromium in CaF_2-SiO_2-Al_2O_3-MgO Flux Applied in Aluminium-Assisted Alloying of Carbon Steel in Submerged Arc Welding. *Minerals* **2022**, *12*, 1397. [CrossRef]
54. Coetsee, T.; De Bruin, F. In Situ Modification of CaF_2-SiO_2-Al_2O_3-MgO Flux Applied in the Aluminium-Assisted Transfer of Titanium in the Submerged Arc Welding of Carbon Steel: Process Mineralogy and Thermochemical Analysis. *Minerals* **2022**, *12*, 604.
55. Hallén, H.; Johansson, K.-E. Use of a Metal Powder for Surface Coating by Submerged Arc Welding. U.S. Patent 6331688 B1, 18 December 2001.
56. Burck, P.A.; Indacochea, J.E.; Olson, D.L. Effects of welding flux additions on 4340 steel weld metal composition. *Weld. J.* **1990**, *69*, 115–122.
57. Lau, T.; Weatherly, G.C.; McLean, A. Gas/Metal/Slag reactions in Submerged Arc Welding using CaO-Al_2O_3 based fluxes. *Weld. J.* **1986**, *65*, 31–38.
58. North, T.H.; Bell, H.B.; Nowicki, A.; Craig, I. Slag/Metal interaction, oxygen and toughness in Submerged Arc Welding. *Weld. J.* **1978**, *57*, 63–75.